ARTICLES

Continuous wavelet transform analysis of one-dimensional quantum bound states from first principles

Carlos R. Handy and Romain Murenzi
Department of Physics and Center for Theoretical Studies of Physical Systems, Clark Atlanta University, Atlanta, Georgia 30314
(Received 26 October 1995; revised manuscript received 13 June 1996)

Over the last decade, Handy and Bessis have developed a moment-problem-based, multiscale quantization theory, the eigenvalue moment method (EMM), which has proven effective in solving singular, strongly coupled, multidimensional Schrödinger Hamiltonians. We extend the scope of EMM by demonstrating its essential role in the generation of wavelet transforms for one-dimensional quantum systems. Combining this with the function-wavelet reconstruction formulas currently available, we are able to recover the wave function systematically, from first principles, through a multiscale process proceeding from large spatial scales to smaller ones. This accomplishment also addresses another outstanding problem, that of reconstructing a function from its moments. For the class of problems considered, the combined EMM-wavelet analysis yields a definitive solution. [S1050-2947(96)02011-2]

PACS number(s): 03.65.Ca, 03.65.Ge, 03.65.Db

I. INTRODUCTION

Over the last ten years, wavelet transform analysis has become a powerful tool in the analysis and synthesis of signals and images [1]. Its main contribution is the definition of a systematic process for identifying and extracting the multiscale features of a signal through simultaneous time and frequency localizations. Despite these successes, recent attempts at applying such methods to the study of linear differential and partial differential equations (ODE's and PDE's), such as the Schrödinger equation with a rational fraction potential, have not proven too successful partly because many of these equations do not admit a tractable wavelet transform representation [2]. Nevertheless, we can circumvent these difficulties by first examining a suitable *moment equation* representation for the given ODE or PDE.

Through the asymptotic analysis methods developed by Blankenbeckler, De Grand, and Sugar (BDS) [3] and further elaborated by Killingbeck, Jones, and Thompson (KJT) [4], the perturbative analysis (reviewed) by Fernandez and Ogilvie [5], Handy's Rayleigh-Ritz variational formulation [6], or the moment problem techniques of Handy and Bessis [7–9], the aforementioned *moment equations* can be solved and used as the starting point for generating the wavelet transform. However, only the latter series of works [referred to as the eigenvalue moment method (EMM)], with their emphasis on *missing moments*, offers a more appropriate formalism for generating the wavelet transform.

We shall combine EMM quantization and wavelet analysis in solving one-dimensional (1D) Schrödinger problems, $-\partial_x^2\Psi(x)+V(x)\Psi(x)=E\Psi(x)$, where the potential function, $V(x)$, can be any rational polynomial. More general potentials are allowed, provided the quantum problem can be transformed [$x\rightarrow y$ and $\Psi(x)\rightarrow\Phi(y)$] into a linear differential equation, $\Sigma_{i=0}^{p}C_i(y)\partial_y^i\Phi(y)=0$, of arbitrary order, with rational fraction coefficients in the new variable, $C_i(y)$.

Multiscale phenomena, and their mathematical characterization, correspond to the interplay of dynamical processes at different scales. Strongly coupled singular systems, whether linear or nonlinear, can exhibit significant multiscale behavior. The development of effective analytical tools by which to understand them is clearly important and necessary. Given the success of wavelet analysis in signal and image processing, as well as the limited number of recent applications to computational quantum physics [10–12], our approach for computing the wavelet transform from first principles, and reconstructing the bound-state quantum wave function, is an essential contribution in assessing the full impact of wavelet-multiscale analysis in quantum physics.

Wavelet analysis

A continuous wavelet transform requires the selection of a wavelet function $\omega(x)$ satisfying $\int_0^\infty[|\tilde{\omega}(k)|^2/k]dk<+\infty$, where $\tilde{\omega}(k)$ is the Fourier transform. In addition, it should have unit normalization, $\int|\omega(x)|^2=1$ [13,14].

The wavelet transform of a one-dimensional signal (wave function), $\Psi(x)$ or $\Psi''(x)$, is given by

$$\omega_t^{(i)}(a,b)\equiv\sqrt{a^{-1}}\int\omega\left(\frac{(x-b)}{a}\right)\partial_x^i\Psi(x)dx, \quad (1.1a)$$

where $a>0$ and b define the scale and translation parameters, respectively, and $i=0$ *or* 2 [13,14]. The recovery of the wave function is possible through the formula

$$\partial_x^i\Psi(x)=\sum_{m,n}\langle\omega_{m,n}(x)|\partial_x^i\Psi(x)\rangle\tilde{\omega}_{m,n}(x), \quad (1.1b)$$

or

$$\partial_x^i \Psi(x) = \sum_{m,n} \langle \tilde{\omega}_{m,n}(x) | \partial_x^i \Psi(x) \rangle \omega_{m,n}(x), \qquad (1.1c)$$

where $\omega_{m,n}(x) = a_0^{-m/2} \omega[(x - n b_0 a_0^m)/a_0^m]$ define a frame (for arbitrary integers m and n), $\tilde{\omega}_{m,n}(x)$ is its dual frame [15].

If $A/B = 1$ the frame is referred to as *tight*, and $\tilde{\omega}_{m,n}(x) = 2/(A+B)\omega_{m,n}(x)$. If the frame is not tight, $A/B \neq 1$, then there are two possibilities [15,16]. The first is to compute the dual frame. For this case, if the frame consists of wavelets [dilations and translations of one mother wavelet, $\omega(x)$], then the dual must be computed for each translation, $\tilde{\omega}_{0,n}$ [16]. Although, in principle, this entails the calculation of an infinite number of functions; in practice only a finite number are used. Despite this, there are some special wavelets, $\omega(x)$, and b_0 parameter values, for which even though the $\omega_{m,n}(x)$ are not close to defining a tight frame, nevertheless all the $\tilde{\omega}_{m,n}(x)$ are dilated versions of one function [16,17].

The second possibility applies to nontight *snug* frames for which $A/B \approx 1$. In this case, one may take the first term in the defining series expansion for $\tilde{\omega}_{m,n}(x)$ [15]. The resulting approximation yields the reconstruction formula (for the case $a_0 = 2$, $b_0 = 1$) [18]

$$\partial_x^i \Psi(x) \approx \frac{2}{A+B} \sum_{m,n} \omega_{m,n}^{(i)} \frac{1}{\sqrt{2^m}} \omega\left(\frac{(x - n2^m)}{2^m} \right), \qquad (1.2)$$

where $\omega_{m,n}^{(i)} \equiv \omega_t^{(i)}(2^m, n2^m)$ for $i = 0$ *or* 2, and $A + B = 6.819$.

One of the more popular wavelet functions is the Mexican hat function, corresponding to $\omega(x) = -\mathcal{N}\partial^2 \exp(-\frac{1}{2}x^2) = \mathcal{N}(1-x^2)\exp(-\frac{1}{2}x^2)$, where $\mathcal{N} = (2/\sqrt{3})\pi^{-(1/4)}$. We shall use this wavelet throughout this work.

The selection of the Mexican hat function wavelet is a matter of convenience. In general, the methods developed here apply to any wavelet of the form $\partial_x^p e^{Q(x)}$, $p \geq 1$, provided $Q(x)$ is a polynomial, and $\lim_{|x| \to \infty}[\partial_x^p e^{Q(x)}] = 0$.

The reconstruction formula in Eq. (1.2) is approximating the wave function through a superposition of localized oscillating structures. The wave function is being approximated in the L^2 norm. Through the eigenvalue moment method discussed in the following section, we will be able to generate a finite number of the $\omega_{m,n}^{(i)}$ coefficients, thereby enabling the approximate reconstruction of the wave function.

It will be noted that an apparent paradox is created by Eq. (1.2), for the case $i = 0$, because the wave function, generally satisfying $\int \Psi(x) dx \neq 0$, is being represented as a superposition of wavelets, each of whose integral is zero, $\int \omega[(x - n2^m)/2^m] dx = 0$. The resolution is that the wavelet-function reconstruction formulas apply in the L^2 norm, not in L^1. Thus, simply integrating both sides of Eq. (1.2) is incorrect. We are still guaranteed pointwise convergence. This ''paradox'' is fully discussed by Daubechies in Ref. [19]. Our numerical results are in keeping with these theoretical observations.

As indicated in Eq. (1.2) for $i = 2$, we also examine the wavelet-reconstruction formula for $\Psi''(x)$. That is, we do not simply determine the second derivative of the wavelet approximant to $\Psi(x)$, but instead determine the wavelet transform for $\Psi''(x)$ directly through the EMM method. This exercize is to demonstrate the consistency of the overall approach advocated.

All of the results are very satisfactory, particularly those related to determining the wavelet approximant for the second-order derivative configurations. We stress once more that our principal objective is to show how EMM theory can be used to generate the $\omega_{m,n}^{(i)}$ coefficients. There are many possible wavelet-reconstruction formulas, some involving Gaussians [10] (the choice $i = 2$ corresponds to this case) as opposed to the Mexican hat wavelets in Eq. (1.2). We only utilize Eq. (1.2) as an example of how to use the generated wavelet coefficients in the reconstruction of the wave function.

II. GENERATING THE $\omega_{m,n}$ THROUGH THE EIGENVALUE MOMENT METHOD

From the preceding discussion, the Mexican hat wavelet transform for the wave function or its second-order derivative [$\partial_x^i \Psi(x)$, for $i = 0$ *or* 2, implicitly assumed hereafter] is given by (after a translation—change of variables):

$$\omega_t^{(i)}(a,b) = \mathcal{N}\sqrt{a^{-1}} \int_{-\infty}^{+\infty} \partial_x^i \Psi(b+x)[1 - (x/a)^2] \times \exp[-\tfrac{1}{2}(x/a)^2] dx, \qquad (2.1)$$

or (defining $\gamma \equiv 1/2a^2$)

$$\omega_t^{(0)}(a,b) = \mathcal{N}(2\gamma)^{1/4}[\mu_{b,\gamma}(0) - 2\gamma\mu_{b,\gamma}(2)] \quad \text{for } i = 0; \qquad (2.2)$$

and

$$\omega_t^{(2)}(a,b) = \mathcal{N}(2\gamma)^{1/4}[-6\gamma\mu_{b,\gamma}(0) + 24\gamma^2\mu_{b,\gamma}(2) - 8\gamma^3\mu_{b,\gamma}(4)] \quad \text{for } i = 2, \qquad (2.3)$$

where

$$\mu_{b,\gamma}(p) \equiv \int_{-\infty}^{+\infty} x^p \Psi(b+x) \exp(-\gamma x^2) dx, \quad p \geq 0 \qquad (2.4)$$

are the Hamburger moments of the measure $\Phi_{b,\gamma}(x) \equiv \Psi(b+x)\exp(-\gamma x^2)$.

The Hamburger moments satisfy the following differential equation with respects to the $\gamma > 0$ variable:

$$\partial_\gamma \mu_{b,\gamma}(p) = -\mu_{b,\gamma}(p+2). \qquad (2.5)$$

For all one-dimensional Schrödinger Hamiltonians with rational fraction potentials (as well as many other types of potentials that can be converted into rational fraction form after a suitable change of variables), all of the Hamburger moments become linearly dependent on the first $1 + m_s$ order *missing moments* [7–9]:

$$\mu_{b,\gamma}(p) = \sum_{j=0}^{m_s} M_{E,b,\gamma}(p,j)\mu_{b,\gamma}(j), \qquad (2.6)$$

where the energy E, dependent coefficients $M_{E,b,\gamma}(p,j)$ are numerically or algebraically determinable, and must satisfy $M_{E,b,\gamma}(i,j)=\delta_{i,j}$ for $0\leqslant i,j\leqslant m_s$ [7–9]. Clearly, inserting Eq. (2.6) into Eq. (2.5) yields a closed set of $1+m_s$ coupled, first-order, linear differential equations

$$\partial_\gamma \mu_{b,\gamma}(i)=-\sum_{j=0}^{m_s} M_{E,b,\gamma}(i+2,j)\mu_{b,\gamma}(j) \quad \text{for } 0\leqslant i\leqslant m_s . \tag{2.7}$$

For arbitrary b, given the physical energy and starting missing moment values $\{\mu_{b,0}(i)|0\leqslant i\leqslant m_s\}$ one can numerically integrate Eq. (2.7) and proceed to determine the wavelet transform [Eqs. (2.2) and (2.3)]. Facilitating this is the relation

$$\mu_{b,0}(p)=\int_{-\infty}^{+\infty} x^p \Psi(b+x)dx=\int_{-\infty}^{+\infty}(x-b)^p\Psi(x)dx, \tag{2.8}$$

or (expanding)

$$\mu_{b,0}(p)=\sum_{q=0}^{p}\binom{p}{q}(-b)^{p-q}\mu_{0,0}(q). \tag{2.9}$$

The physical values for the energy E and $\mu_{0,0}(q)\equiv\int_{-\infty}^{+\infty}x^q\Psi(x)$ Hamburger moments, for $0\leqslant q\leqslant m_s$, are determined by the eigenvalue moment method (discussed in Sec. III). In practice, for each pair of values $(a=2^m, b=n2^m)$ at each point $b=n2^m$ we integrate Eq. (2.7) up to $\gamma=\frac{1}{2}a^{-2}=\frac{1}{2}2^{-2m}$, which then allows us to generate the wavelet transform coefficients $\omega_{m,n}^{(i)}$.

An important observation is that the asymptotic behavior of the $\mu_{b,\gamma}(p)$ moments, with respect to $\gamma\to\infty$, determines the wave function:

$$\lim_{\gamma\to+\infty}\mu_{b,\gamma}(p)=\left(\frac{1}{\sqrt{\gamma}}\right)^{(p+1)}\theta(p/2)\Psi(b), \quad p=\text{even} \tag{2.10}$$

where $\theta(\rho)=\int_{-\infty}^{+\infty}y^{2\rho}\exp(-y^2)dy$. For $p=0,2$, we have $\theta(0)=\sqrt{\pi}$ and $\theta(1)=\sqrt{\pi}/2$. As will be clarified in Sec. III, an implicit normalization is assumed in the implementation of the EMM quantization. Our numerical comparisons between the wavelet-reconstructed wave function and the actual wave function (obtained from direct integration of the Schrödinger equation) will assume $\Psi(0)$ to have the value generated through Eq. (2.10) (approximated by a sufficiently large γ value).

III. OVERVIEW OF THE EIGENVALUE MOMENT METHOD

We briefly outline the essentials of EMM theory, as related to the wavelet problem at hand, through the quartic anharmonic-oscillator Hamiltonian. As previously noted, our methods are applicable to arbitrary one-dimensional quantum systems with rational fraction potentials (or more general potentials that can be transformed into rational fraction form). A more detailed explanation of EMM theory may be found in the cited references.

The quartic anharmonic potential problem is defined by

$$-\frac{d^2\Psi}{dx^2}+(mx^2+gx^4)\Psi(x)=E\Psi(x). \tag{3.1}$$

Bearing in mind the formalism in Sec. II, we need to define a moment equation for the configuration $\Phi_{b,\gamma}(x)\equiv\Psi(b+x)\exp(-\gamma x^2)$. One first obtains the differential equation:

$$\left[-\left(\frac{d^2}{dx^2}+4\gamma x\frac{d}{dx}+2\gamma+4\gamma^2x^2\right)+[m(x+b)^2+g(x+b)^4]\right]\Phi_{b,\gamma}(x)=E\Phi_{b,\gamma}(x). \tag{3.2}$$

The Hamburger moments, $\mu_{b,\gamma}(p)=\int x^p\Psi(b+x)\exp(-\gamma x^2)dx$, satisfy the moment equation (for $p\geqslant 0$)

$$\mu_{b,\gamma}(p+4)=\sum_{i=1}^{3}C_i[\gamma]\mu_{b,\gamma}(p+i)+\left\{-4\frac{\gamma p}{g}+C_0[\gamma]\right\}\times\mu_{b,\gamma}(p)+\frac{p(p-1)}{g}\mu_{b,\gamma}(p-2), \tag{3.3}$$

where the coefficients are $C_3=-4b$, $C_2[\gamma]=g^{-1}[4\gamma^2-m-6gb^2]$, $C_1=-g^{-1}[2bm+4gb^3]$, and $C_0[\gamma]=-g^{-1}[2\gamma+mb^2+gb^4-E]$.

The moment equation corresponds to a linear, homogeneous, fourth-order finite-difference equation (for nonnegative p values). All of the moments are linearly dependent on the initialization or missing moments $\{\mu_{b,\gamma}(i)|0\leqslant i\leqslant 3\}$. This is expressed through the relation

$$\mu_{b,\gamma}(p)=\sum_{j=0}^{3}M_{E,b,\gamma}(p,j)\mu_{b,\gamma}(j), \tag{3.4a}$$

where

$$M_{E,b,\gamma}(i,j)=\delta_{i,j} \quad \text{for } 0\leqslant i, \quad j\leqslant 3, \tag{3.4b}$$

and the remaining $M_{E,b,\gamma}(p>3,j)$ coefficients satisfy the same moment equation as in Eq. (3.3).

The relation [from Eq. (2.5)]

$$\frac{\partial}{\partial\gamma}\begin{pmatrix}\mu_{b,\gamma}(0)\\ \mu_{b,\gamma}(1)\\ \mu_{b,\gamma}(2)\\ \mu_{b,\gamma}(3)\end{pmatrix}=-\begin{pmatrix}\mu_{b,\gamma}(2)\\ \mu_{b,\gamma}(3)\\ \mu_{b,\gamma}(4)\\ \mu_{b,\gamma}(5)\end{pmatrix} \tag{3.5}$$

now becomes [upon substituting Eq. (3.4a)]

$$\frac{\partial}{\partial\gamma}\begin{pmatrix}\mu_{b,\gamma}(0)\\ \mu_{b,\gamma}(1)\\ \mu_{b,\gamma}(2)\\ \mu_{b,\gamma}(3)\end{pmatrix}=\begin{pmatrix}0 & 0 & -1 & 0\\ 0 & 0 & 0 & -1\\ \mathcal{M}_{2,0}[\gamma] & \mathcal{M}_{2,1}[\gamma] & \mathcal{M}_{2,2}[\gamma] & \mathcal{M}_{2,3}[\gamma]\\ \mathcal{M}_{3,0}[\gamma] & \mathcal{M}_{3,1}[\gamma] & \mathcal{M}_{3,2}[\gamma] & \mathcal{M}_{3,3}[\gamma]\end{pmatrix}\begin{pmatrix}\mu_{b,\gamma}(0)\\ \mu_{b,\gamma}(1)\\ \mu_{b,\gamma}(2)\\ \mu_{b,\gamma}(3)\end{pmatrix} \tag{3.6}$$

[note that $\mathcal{M}_{2,0\leqslant j\leqslant 3}=-M_{E,b,\gamma}(4,j)$ and $\mathcal{M}_{3,0\leqslant j\leqslant 3}=-M_{E,b,\gamma}(5,j)$], where $\mathcal{M}_{2,0}[\gamma]=-C_0[\gamma]$, $\mathcal{M}_{2,1}[\gamma]=-C_1$, $\mathcal{M}_{2,2}[\gamma]=-C_2[\gamma]$, $\mathcal{M}_{2,3}[\gamma]=-C_3$, $\mathcal{M}_{3,0}[\gamma]=-C_0[\gamma]C_3$, $\mathcal{M}_{3,1}[\gamma]=-(C_1C_3+C_0[\gamma]-4\gamma/g)$, $\mathcal{M}_{3,2}[\gamma]=-(C_1+C_3C_2[\gamma])$, and $\mathcal{M}_{3,3}[\gamma]=-(C_2[\gamma]+C_3^2)$.

As indicated in the previous sections, given the starting values for the missing moments, $\{\mu_{b,\gamma=0}(i),(0\leqslant i\leqslant 3)\}$, at any b, one can integrate the above equations. Facilitating the determination of these starting moment values is the relation in Eq. (2.9). Accordingly, one must determine the physical energy E and the physical missing moment values $\{\mu_{b=0,\gamma=0}(i),(0\leqslant i\leqslant 3)\}$.

The $\mu_{0,0}(p)$ moments satisfy the moment equation

$$\mu_{0,0}(p+4)=g^{-1}[-m\mu_{0,0}(p+2)+E\mu_{0,0}(p)+p(p-1)\mu_{0,0}(p-2)], \tag{3.7}$$

for $p\geqslant 0$. Symmetric configurations, such as the ground state, will have all their odd-order moments equal to zero, $\mu_{0,0}(\text{odd})=0$. For such configurations, one can streamline the formalism and effectively work with the even-order Stieltjes moments $u(\rho)\equiv\mu_{0,0}(2\rho)$. Accordingly, only $u(0)$ and $u(1)$ become the nonzero missing moments in this case. An analogous formulation is possible for antisymmetric configurations; however, for simplicity, these are not discussed in this work.

The homogeneous nature of the moment equation implies the necessity for some normalization condition. One convenient choice is

$$u(0)+u(1)=1. \tag{3.8}$$

Eliminating $u(0)$, all of the moments become linearly dependent on the unconstrained missing moment $u(1)$. This may be expressed through the relation $u(\rho)=\hat{M}_E(\rho,0)+\sum_{j=1}^{1}\hat{M}_E(\rho,j)u(j)$, where the $\hat{M}_E$ coefficients are readily determinable from Eq. (3.4) and the above normalization.

The EMM quantization procedure involves making use of the positivity properties of the associated wave function in order to define constraints on the physically allowed energy and missing moment values. For the ground-state wave function, the fact that $\Psi_{\text{ground}}(x)>0$ [20], allows us to impose the Hankel-Hadamard, nonlinear, determinantal constraints on the E parameter and missing-moment variables [21,22]:

$$\Delta_{m,n}[E,u(1)]>0 \quad \text{for } m=0,1 \quad \text{and } n\geqslant 0, \tag{3.9a}$$

where

$$\Delta_{m,n}\equiv\text{Det}\begin{pmatrix}u(m) & u(m+1) & \cdots & u(m+n)\\ u(m+1) & u(m+2) & \cdots & u(m+n+1)\\ \vdots & \vdots & \cdots & \vdots\\ u(m+n) & u(m+n+1) & \cdots & u(m+2n)\end{pmatrix}, \tag{3.9b}$$

and each of the Stieltjes moments $u(\rho)$ is implicitly dependent on the energy parameter E and the unconstrained missing moment $u(1)\equiv\mu_{0,0}(2)$.

The algorithmic implementation of EMM theory is discussed in Refs. [8,9] and entails the use of linear programming [23] to determine the E values admitting missing-moment solution sets to the above inequalities. Implementation of this procedure for the ground state yields the ground-state energy and missing-moment values (for $g=m=1$) $E=1.392\ 351\ 641\ 53$, $u(0)=0.642\ 670\ 622\ 325$, and $u(1)=0.357\ 329\ 377\ 675$. As a side note, it is important to emphasize that the EMM approach generates converging lower and upper bounds to the ground-state energy, as well as the missing-moment values (not given here); therefore, it is a very reliable computational theory since one can accurately assess the quality of the computed results.

Utilizing the above (ground-state) energy and missing-moment values, one can then use Eq. (2.9) to recover, for arbitrary b, the starting missing-moment values $\mu_{b,0}(0-3)$ in the integration of Eq. (3.6). We used a fourth-order Runge-Kutta procedure [24]. In general, for $|b|<5$, we could integrate over γ up to an order $\gamma<O(10^2)$. Beyond this γ value, one (or both) of the two even-order moments, $\mu_{b,\gamma}$ (2 and 4), no longer remained positive (which they must be). More precisely, in our numerical integration of Eq. (3.6) the integration iterates, $\{\mu_{\gamma_l,b}(p)|0\leqslant p\leqslant 3\}$, for $\gamma_l\equiv l\,\delta\gamma$ (for integer l and $\delta\gamma=10^{-4}$, were sampled at every Lth step ($\Delta l=L$, $L\leqslant 10$) to ascertain if the $\mu_{\gamma l,b}(0)$ and $\mu_{\gamma l,b}(2)$ moments were strictly decreasing. For $\gamma>O(10^2)$ our integration procedure yielded a violation of the latter condition.

Taking into account the above, we could only generate the wavelet coefficients $\omega_{m,n}$ corresponding to m, n integer values $|n2^m|<5$ and $\frac{1}{2}(2^m)^{-2}<O(10^2)$ [i.e., $\gamma=\frac{1}{2}a^{-2}<O(10^2)$]. Specifically, we took $-3\leqslant m\leqslant 3$.

One can compare the numerically observed limiting values for the asymptotic limits $\lim_{\gamma\to\infty}\sqrt{\gamma/\pi}\,\mu_{b,\gamma}(0)$ and $\lim_{\gamma\to\infty}(2\gamma^{3/2}/\sqrt{\pi})\mu_{b,\gamma}(2)$. According to Eq. (2.10), they both must approach $\Psi(b)$. In Table I we compare these (approximate) limits obtained from the numerical integration of Eq. (3.6). In our Runge-Kutta integration, for $|b|\leqslant 2.5$ there was reasonable agreement between these two estimates (becoming progressively better as $b\to 0$), indicating that at γ values approximately $O(10^2)$ the asymptotic limit was attained. Therefore, we used these numerical estimates for the

TABLE I. $\Psi(b)$ Estimates from Eq. (2.10). [n] denotes power of 10.

b	γ	$\sqrt{\frac{\gamma}{\pi}}\,\mu_{b,\gamma}[0]$	$\frac{2\gamma^{3/2}}{\sqrt{\pi}}\,\mu_{b,\gamma}[2]$
5	3.2	0.17[−10]	0.27[−9]
4.5	3.2	0.32[−8]	0.51[−7]
4	3.4	0.21[−6]	0.25[−5]
3.5	3.5	0.86[−5]	0.80[−4]
3	3.8	0.18[−3]	0.98[−3]
2.5	81.1	0.43[−3]	0.54[−3]
2	81.6	0.74[−2]	0.82[−2]
1.5	82.1	0.49[−1]	0.50[−1]
1	82.6	0.151 408[0]	0.151 953[0]
.5	83.1	0.272 213[0]	0.270 469[0]
0	83.6	0.325 230[0]	0.322 563[0]

asymptotic limit at $b=0$, in order to define the $\Psi(0)$ value. In other words, the adopted moment normalization in Eq. (3.8), combined with the asymptotic formulas in Eq. (2.10), require that the corresponding ground-state wave function satisfy $\Psi_{\text{ground}}(0)\approx 0.325$ $(g=m=1)$. This value can then also be used to integrate the wave function directly from the Schrödinger equation (using the EMM ground-state energy estimate given above), through a fourth-order Runge-Kutta ansatz.

Three results are illustrated in Fig. 1: (i) the Ψ_{ground} estimate given from Eq. (2.10) for the $p=0,2$ cases (Table I); (ii) the direct Runge-Kutta integration of the ground-state wave function from the Schrödinger equation [utilizing the $\Psi(0)=0.325$ value given from Table I]; and (iii) the Mexican hat function wavelet–wave function reconstruction utilizing the formula in Eq. (1.2) ($i=0$ case). With respects to the latter, we show the effect of the wavelet reconstruction when successive smaller scales are included. Thus, $m\geqslant m_n$ means that only the corresponding terms in Eq. (1.2) were used in generating the wavelet approximant. In Fig. 1, the cases $m_n=-3$ and $m_n=-2$ lie too close for graphing purposes. As such, the latter is not shown. In general, all of the results in Fig. 1 are very good. Of course, the asymptotic estimates from Eq. (2.10) are exceptionally good.

A similar analysis was carried out for $\Psi''(x)$. That is, we generated its Mexican hat wavelet transform coefficients and used Eq. (1.2) (for $i=2$) to recover $\Psi''(x)$. This also involves using Eq. (3.8). We compared the wavelet reconstructed configuration to that generated by direct integration of the Schrödinger equation [taking $\Psi''(x)=(mx^2+gx^4-E)\Psi(x)$]. The results of this analysis are given in Fig. 2. The wavelet results are much better than those in Fig. 1. The wavelet approximant corresponding to $m\geqslant -3$ is not shown because the results were very poor compared to the true solution. We suspect that numerical integration errors for large γ values [$\gamma\approx O(10^2)$] are amplified by the γ^3 factor in Eq. (2.3), therefore yielding poorer estimates for the wavelet transform coefficients $\omega^{(2)}_{m,n}$ at larger γ values (or alternatively, algebraically smaller m values).

In principle, one need not use the EMM method to initiate the Runge-Kutta integration of Eq. (3.6). It is possible to use the asymptotic arguments of BDS [3] and KJT [4] instead, as indicated at the outset. However, their formalism does not emphasize the missing-moment structure essential to the preceding analysis. In addition, while the analysis of BDS is a little less speculative than that of KJT, who also focus on perturbative analysis of the moment equations with respect to the coupling constant g (in this regard, also refer to the works of Witwit [25]), the former's asymptotic methods may not be practical in general, particularly for multidimensional problems. None of these difficulties is encountered in the EMM formulation (or its Rayleigh-Ritz counterpart discussed in Ref. [6]), which is rigorously based on fundamental theorems in mathematics and mathematical physics, as well as on innovative applications of linear programming optimization theory (in order to solve the nonlinear Hankel-Hadamard moment constraints). In addition, the EMM approach automatically gives lower and upper bounds to the physical energy as well as missing-moment values, making it a very reliable computational procedure.

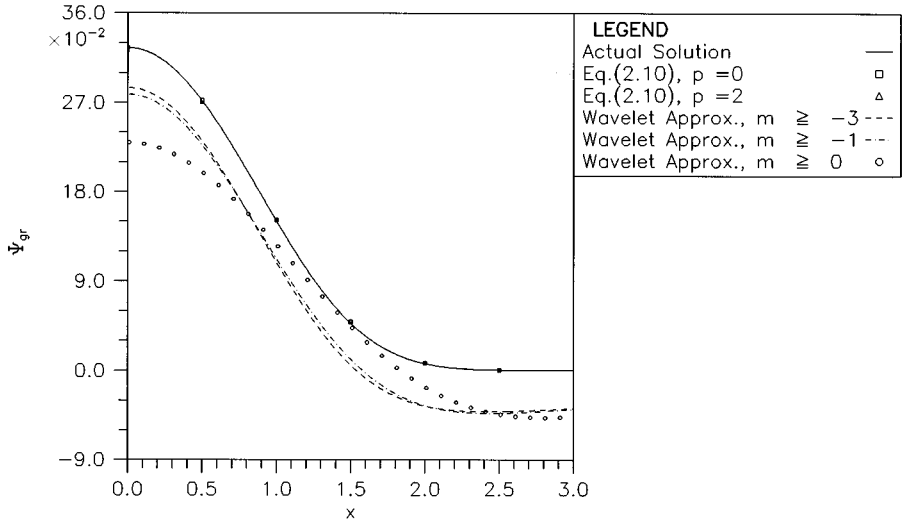

FIG. 1. $\Psi_{\text{ground}}(x)$, $V(x)=x^2+x^4$.

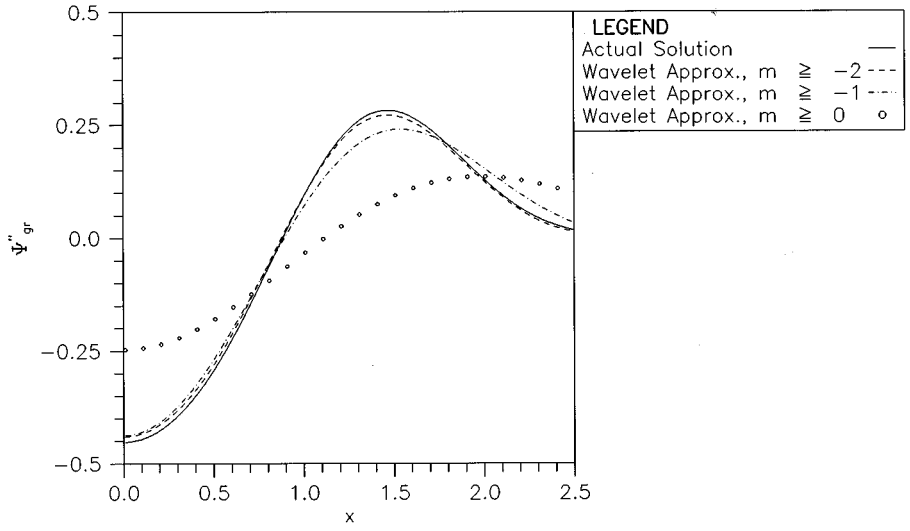

FIG. 2. $\partial_x^2\Psi_{\text{ground}}(x)$, $V(x)=x^2+x^4$.

IV. EXTENSION TO EXCITED STATES

The EMM quantization methodology is a multiscale theory appropriate for global problems such as computing (low-lying) eigenenergies. The spatially extensive nature of moments makes them highly effective in this regard, as evidenced by the numerous successful applications of EMM theory in the cited references [7–9]. EMM quantization is achieved by addressing the large- (important) scale dynamics of a system and then progressively focusing on the smaller- (less important) scale contributions. Through the differential equations in Eq. (3.6), as well as the asymptotic relations in Eq. (2.10), there then ensues a multiscale recovery of the local structure of the wave function. Of course, the wavelet-function reconstruction formula [Eq. (2.1)] is an alternate, and effective, way of representing this. For one-dimensional problems of the type exemplified in the preceding analysis, the fundamental role moment quantization plays in wavelet–wave-function multiscale reconstruction motivates its extension to low-lying excited states.

We will extend the EMM-wavelet analysis to low-lying excited states. All of the previous formalism transfers over to this case; however, because of certain essential modifications to the EMM formalism as applied to excited states, we make explicit all the modifications to the previously developed relations. Again, for simplicity, we only consider symmetric excited configurations $\Psi(x)$. A formulation analogous to that presented below can be developed for antisymmetric excited states.

Since the excited state $\Psi(x)$ cannot have a uniform signature (i.e., cannot be uniformly positive), it is necessary to work in an alternate representation in which the corresponding configuration is positive [26]. Thus consider

$$\Upsilon_{\alpha,c}(x)\equiv[\Psi(x)+c]\exp(-\alpha x^2), \tag{4.1}$$

where α is an arbitrary positive parameter and c is some sufficiently positive constant yielding a positive configuration, $\Upsilon_{\alpha,c}(x)>0$, for the excited state of interest. The constant c will be determined through application of the EMM theory. The selection of the Gaussian function, $\exp(-\alpha x^2)$, is done in accordance with the EMM quantization requirements stipulated in Ref. [26]. For the quartic anharmonic-oscillator problem, one may choose it as an appropriate, and simple, regulating function. It is assumed in the immediate discussion that follows that α and c have been determined through the necessary EMM analysis. Our objective is to extend the relations in Sec. III to the $\Upsilon_{\alpha,c}(x)$ configuration. The essentials of the necessary underlying EMM analysis are clarified thereafter.

Let us define

$$\Phi_{\alpha,c,b,\gamma}(x)\equiv\Upsilon_{\alpha,c}(b+x)\exp(-\gamma x^2). \tag{4.2}$$

The corresponding Schrödinger equation is

$$\begin{aligned}-\Phi''_{\alpha,c,b,\gamma}+C_1(x)\Phi'_{\alpha,c,b,\gamma}+C_0(x)\Phi_{\alpha,c,b,\gamma}\\ =c[m(x+b)^2+g(x+b)^4-E]\\ \times\exp[-\alpha(x+b)^2-\gamma x^2],\end{aligned} \tag{4.3}$$

where $C_1(x)=-4[(\alpha+\gamma)x+\alpha b]$, $C_0(x)=C_{0,0}+C_{0,1}x+C_{0,2}x^2+4bgx^3+gx^4$, $C_{0,0}=t_0-2(\alpha+\gamma)-4(\alpha b)^2$, $C_{0,1}=-8\alpha b(\alpha+\gamma)+t_1$, $C_{0,2}=t_2-4(\alpha+\gamma)^2$, $t_0=mb^2+gb^4-E$, $t_1=2bm+4gb^3$, and $t_2=m+6gb^2$.

The moment equation for the $\mu_{\alpha,c,b,\gamma}(p)=\int_{-\infty}^{+\infty}x^p\Phi_{\alpha,c,b,\gamma}(x)$ Hamburger moments is

$$g\mu_{\alpha,c,b,\gamma}(p+4)+4bg\mu_{\alpha,c,b,\gamma}(p+3)+C_{0,2}\mu_{\alpha,c,b,\gamma}(p+2)+C_{0,1}\mu_{\alpha,c,b,\gamma}(p+1)+[C_{0,0}+4(p+1)(\alpha+\gamma)]\mu_{\alpha,c,b,\gamma}(p)$$
$$+4b\alpha p\mu_{\alpha,c,b,\gamma}(p-1)-p(p-1)\mu_{\alpha,c,b,\gamma}(p-2)=c[t_0\eta(p)+t_1\eta(p+1)+t_2\eta(p+2)+4bg\eta(p+3)+g\eta(p+4)]. \tag{4.4}$$

The expression $\eta(p)$ corresponds to the Hamburger moments

$$\eta(p)=\int_{-\infty}^{+\infty}x^p\exp[-\alpha(x+b)^2-\gamma x^2]dx$$
$$=\exp\left(-\alpha b^2+\frac{(\alpha b)^2}{\alpha+\gamma}\right)\sum_{\rho=0}^{p}\binom{p}{\rho}$$
$$\times\left(-\frac{\alpha b}{\alpha+\gamma}\right)^{p-\rho}v(\rho), \tag{4.5}$$

where $v(\rho)=\int_{-\infty}^{+\infty}x^\rho\exp[-(\alpha+\gamma)x^2]dx$ satisfies the recursion relation $v(\rho+2)=[(\rho+1)/2(\alpha+\gamma)]v(\rho)$, with $v(0)=\sqrt{\pi/(\alpha+\gamma)}$ [note that $v(\text{odd})=0$].

The wavelet-transform formula for the $\Upsilon_{\alpha,c}(x)$ configuration is also given by Eqs. (2.2) and (2.3) with respect to the corresponding Hamburger moments $\mu_{\alpha,c,b,\gamma}(p)$. Proceeding as in Sec. III we need to define the missing-moment structure for the present problem. From Eq. (4.4) it is clear that because of the inhomogeneous nature of the moment equation one has

$$\mu_{\alpha,c,b,\gamma}(p)=\sum_{j=0}^{3}M_{E,\alpha,b,\gamma}(p,j)\mu_{\alpha,c,b,\gamma}(j)+cI_{E,\alpha,b,\gamma}(p), \tag{4.6}$$

where the missing moments $\mu_{\alpha,c,b,\gamma}(j\leqslant 3)$ and c are to be regarded as independent variables, and the M coefficients must satisfy $M_{E,\alpha,b,\gamma}(i,j)=\delta_{i,j}$ for $0\leqslant i,j\leqslant 3$ together with $I_{E,\alpha,b,\gamma}(j\leqslant 3)=0$. Under these conditions, inserting Eq. (4.6) into Eq. (4.4) one can easily obtain recursive formulas for the M's and I's.

From the representation

$$\mu_{\alpha,c,b,\gamma}(p)=\int_{-\infty}^{+\infty}x^p\Upsilon_{\alpha,c}(b+x)\exp(-\gamma x^2)$$

it follows that

$$\partial_\gamma\mu_{\alpha,c,b,\gamma}(p)=-\mu_{\alpha,c,b,\gamma}(p+2),$$

or, in terms of Eq. (4.6),

$$\partial_\gamma\mu_{\alpha,c,b,\gamma}(p)=-\left[\sum_{j=0}^{3}M_{E,\alpha,b,\gamma}(p+2,j)\mu_{\alpha,c,b,\gamma}(j)\right.$$
$$\left.+cI_{E,\alpha,b,\gamma}(p+2)\right]. \tag{4.7a}$$

We may limit p to the missing-moment values, thus transforming Eq. (4.7a) into a coupled, inhomogeneous linear equation for the γ-dependent missing moments:

$$\partial_\gamma\mu_{\alpha,c,b,\gamma}(i)=-\left[\sum_{j=0}^{3}M_{E,\alpha,b,\gamma}(i+2,j)\mu_{\alpha,c,b,\gamma}(j)\right.$$
$$\left.+cI_{E,\alpha,b,\gamma}(i+2)\right], \tag{4.7b}$$

for $0\leqslant i\leqslant 3$.

The starting missing-moment values [in the integration of Eq. (4.7b)] are given by

$$\mu_{\alpha,c,b,\gamma=0}(p)=\int_{-\infty}^{+\infty}x^p\Upsilon_{\alpha,c}(b+x)dx$$
$$=\int_{-\infty}^{+\infty}(x-b)^p\Upsilon_{\alpha,c}(x)dx$$

or

$$\mu_{\alpha,c,b,\gamma=0}(p)=\sum_{q=0}^{p}\binom{p}{q}(-b)^{p-q}\mu_{\alpha,c,0,0}(q), \tag{4.8}$$

where the $\mu_{\alpha,c,0,0}(q)$ moments are determined by application of the (c-shift) EMM method, clarified below [26]. For future reference, denote the even-order Hamburger moments as $\mu_{\alpha,c,0,0}(2\rho)\equiv\chi_{\alpha,c}(\rho)\equiv u_\alpha(\rho)+c\,\theta_\alpha(\rho)$, where $u_\alpha(\rho)=\int_{-\infty}^{+\infty}x^{2\rho}\Psi(x)\exp(-\alpha x^2)dx$ and $\theta_\alpha(\rho)=\int_{-\infty}^{+\infty}x^{2\rho}\exp(-\alpha x^2)dx$. The corresponding odd-order Hamburger moments are necessarily zero, since $\Upsilon_{\alpha,c}(x)$ is a symmetric configuration.

In the case of the quartic anharmonic-oscillator problem, the unnormalized missing moments are $\chi_{\alpha,c}(0)$ and $\chi_{\alpha,c}(1)$. Imposing the normalization $u_\alpha(0)+u_\alpha(1)=1$ yields the relation $\chi_{\alpha,c}(0)+\chi_{\alpha,c}(1)=1+c[\theta_\alpha(0)+\theta_\alpha(1)]$. If c is chosen so that $c>c_{\min}$ (as clarified below), then the physical moment values must satisfy $\chi_{\alpha,c}(\rho)>0$ and thus $0<\chi_{\alpha,c}(1)<1+c[\theta_\alpha(0)+\theta_\alpha(1)]$. After the necessary substitutions are made in Eq. (4.6) (for $b=\gamma=0$), it then follows that

$$\chi_{\alpha,c}(\rho)=\hat{M}_{E,\alpha}(\rho,0)+\sum_{j=1}^{1}\hat{M}_{E,\alpha}(\rho,j)\chi_{\alpha,c}(j)$$
$$+c\hat{I}_{E,\alpha}(\rho),\quad \rho\geqslant 0, \tag{4.9}$$

where the $\hat{M}$ and $\hat{I}$ coefficients are obtainable from the M and I coefficients in Eq. (4.6).

Quantization of the desired excited state ensues if for a given α value a sufficiently positive c value can be found for which there exists an E and $\chi_{\alpha,c}(1)$ solution set to the positivity conditions for the associated Hankel-Hadamard moment determinantal inequalities [26]:

$$\Delta_{m,n}[E,c,\chi_{\alpha,c}(1)]>0 \quad \text{for } m=0,1 \quad \text{and } n\geqslant 0. \tag{4.10}$$

As in the ground-state case, linear programming methods can be used to determine the E and c values admitting a missing-moment solution set to these inequalities. As the number of inequalities increases, $m+2n\leqslant N\rightarrow\infty$, the EMM-generated lower and upper bounds, $E^N_{\text{lower}}<E^{\text{exc}}<E^N_{\text{upper}}$, $\chi^N_{\text{lower};\alpha,c}<\chi^{\text{exc}}_{\alpha,c}<\chi^N_{\text{upper};\alpha,c}$, converge to the physical excited-state values, E^{exc} and $\chi^{\text{exc}}_{\alpha,c}$, so long as $c>c_{\min}$. The latter quantity $c_{\min}$ is not actually determined; however, it exists and must satisfy $c_{\min}>0$. Only if the chosen c value is greater than $c_{\min}$ will the generated lower and upper bounds converge to the physical values. If c is chosen so that $c<c_{\min}$, then either (i) no E, $\chi_{\alpha,c}$ solution set can be found, or (ii) if for some N a solution set is found, then as $N\rightarrow\infty$ the solution set disappears.

The result of implementing the above EMM analysis with respect to the first excited symmetric state ($g=m=1$ and $\alpha=1$, $c=3$) is

$$E^{\text{exc}}=8.655\,049\,962\,363,$$

$$\mu^{\text{exc}}_{\alpha,c,0,0}(0)=5.030\,896\,702,$$

and

$$\mu^{\text{exc}}_{\alpha,c,0,0}(2)=3.945\,145\,627,$$

where $\mu^{\text{exc}}_{\alpha,c,0,0}(1)=\mu^{\text{exc}}_{\alpha,c,0,0}(3)=0$. These physical values are then used to calculate the $\mu_{\alpha,c,b,0}(0-3)$ moments, for arbitrary b [Eq. (4.8)], which are the initial moment values in the integration of Eq. (4.7b).

As for the ground-state wave function, the corresponding relation to Eq. (2.10) also is valid:

$$\lim_{\gamma\rightarrow+\infty}\mu_{\alpha,c,b,\gamma}(p)=\left(\frac{1}{\sqrt{\gamma}}\right)^{(p+1)}\theta(p)\Upsilon_{\alpha,c}(b), \quad p=\text{even}. \tag{4.11}$$

Utilizing this asymptotic relation, as in the ground-state wave-function case, we can test where, and how well, γ asymptotic limit is reached. In Table II we give the estimate for $\Psi^{\text{exc}}(b)$ calculated from the preceding asymptotic relations $[\Psi^{\text{exc}}(b)=\Upsilon_{\alpha,c}\exp(\alpha x^2)-c]$.

It will be noted that the wave-function values in Table II do reflect the signature structure expected for the excited state. In Fig. 3 we plot the results of Table II together with the Runge-Kutta integration of the Schrödinger equation, utilizing the $\Psi^{\text{exc}}(0)$ value in Table II. We also plot the Mexican hat wavelet–wave-function reconstruction [Eq. (1.2)]. The results are reasonably good. It will be noted that the $m\geqslant -3$ and $m\geqslant -2$ results lie very close to one another (both represented with the same line type). The $m\geqslant -2$ wavelet approximant lies above the $m\geqslant -3$ at $x=0$.

In Fig. 4 we plot the results of a wavelet–wave-function reconstruction for $\partial_x^2\Psi^{\text{exc}}(x)$ as well as the result of direct integration of the Schrödinger equation. Once again, the results are much better than those in Fig. 3.

The implementation of the numerical integration for the excited state was the same as for the ground state. Our simple implementation of a fourth-order Runge-Kutta integration limited us to $\gamma<O(10^2)$. As such, in the generation of the wavelet-transform coefficients $\omega_{m,n}$ for $a=2^m$ and $b=n2^m$ (m,n being arbitrary negative and positive integers), the integers are restricted to $-3\leqslant m\leqslant 3$ and $|n2^m|<5$ (recall that $\gamma=\frac{1}{2}a^{-2}$). As in the case of Fig. 2, we suspect that amplification of the numerical integration errors led to poor wavelet-transform coefficients for $\omega^{(2)}_{m=-3,n}$. The corresponding wavelet approximant to $\Psi''(x)$ did not agree well with the true solution. As such, only the $m\geqslant -2$ cases are shown.

TABLE II. Estimates for $\Psi^{\text{exc}}(b)$ from Eq. (4.11). [n] denotes power of 10.

b	γ	Eq. (4.11), $p=0$	Eq. (4.11), $p=2$
2.5	80.0	0.27 [0]	0.75 [0]
2	80.5	0.64 [0]	0.11 [+1]
1.8	80.5	0.11 [+1]	0.15 [+1]
1.6	81.0	0.17 [+1]	0.20 [+1]
1.5	81.0	0.20 [+1]	0.23 [+1]
1.4	81.0	0.22 [+1]	0.23 [+1]
1.3	81.0	0.24 [+1]	0.26 [+1]
1.2	81.0	0.25 [+1]	0.26 [+1]
1.1	81.5	0.249 908 [+1]	0.248 174 [+1]
1	81.5	0.233 271 [+1]	0.224 852 [+1]
0.9	81.5	0.201 977 [+1]	0.188 888 [+1]
0.8	81.5	0.157 071 [+1]	0.141 749 [+1]
0.7	81.5	0.101 056 [+1]	0.860 279 [0]
0.6	82.0	0.377 355 [0]	0.253 543 [0]
0.5	82.0	−0.282 880 [+0]	−0.364 205 [0]
0.4	82.0	−0.918 045 [0]	−0.947 493 [0]
0.3	82.0	−0.147 679 [+1]	−0.145 375 [+1]
0.2	82.0	−0.191 304 [+1]	−0.184 531 [+1]
0.1	82.5	−0.219 067 [+1]	−0.209 356 [+1]
0	83.6	−0.228 582 [+1]	−0.217 832 [+1]

To avoid confusion, we repeat that we used the above moment-wavelet formalism to generate the wavelet-transform coefficients for the excited-state configuration $\partial_x^2\{[\Psi(x)+c]\exp(-\alpha x^2)\}\equiv S(x)$. Using the Mexican hat approximation to $S(x)$, $S_{mw}(x)$, we then recovered the approximate $\Psi''(x)$ by using $\Psi''(x)\approx S_{mw}(x)\exp(\alpha x^2)+4\alpha x\Psi'(x)-\{\Psi(x)+c\}[-2\alpha+4\alpha^2x^2]$. The values for $\Psi'(x)$ and $\Psi(x)$ used were those obtained from direct numerical integration of the Schrödinger equation. We could have approximated them instead by their respective wavelet approximants; however, for expediency, we chose not to do so.

V. CLOSING REMARKS

It has been shown that a moment quantization approach based on the EMM formalism defines a systematic multiscale analysis (proceeding from large spatial scales to small spatial scales) for determining not only the global properties of the system (eigenenergies, moments, etc.) but also the local structure of the wave function. Furthermore, for wavelet transforms that can be simply related to moments [refer to Eqs. (2.2) and (2.3)], the EMM philosophy plays a vital role in the determination of the wavelet transform at all scales,

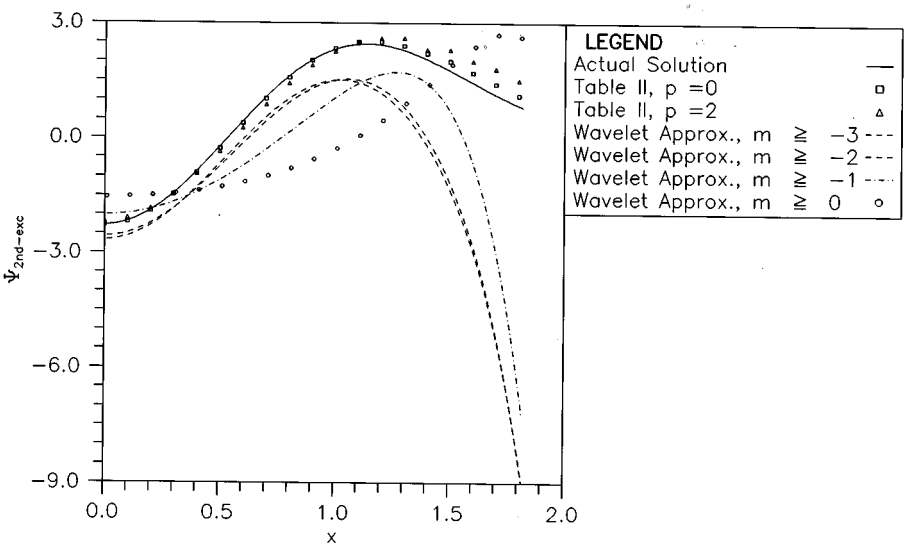

FIG. 3. $\Psi_{\text{2nd-exc}}(x)$, $V(x)=x^2+x^4$.

and in the approximation of the wave function through the use of wavelet–wave-function reconstruction formulas.

Our numerical integration methods are not the most robust. Application of more advanced numerical integration methods easily extended our Runge-Kutta results to larger γ values $[O(10^3)]$ than those quoted in Tables I and II. However, the preliminary numerical results given here clearly demonstrate the practical benefits of a combined EMM-wavelet analysis in systematically analyzing the multiscale structure of low-lying bound states.

As indicated at the outset, EMM quantization is not the only moment-equation-representation quantization theory. Its use in this work is due to the fact that because it can generate tight eigenenergy bounds [as well as bounds for the input missing moment values in Eq. (3.5)], there is greater confidence in the numerical integration results. Complementing the alternate moment-equation quantization methods cited in the present work (i.e., Refs. [3–5]), another such approach [6] has been recently developed in which the missing moments become the variational parameters in an effective Fourier-space Rayleigh-Ritz variational ansatz. The method is easy to apply and yields excellent results for the ground state.

Finally, this work clearly addresses another important problem, the recovery of a function from knowledge of its moments. Given the moments and energy of a low-lying bound-state solution to the Schrödinger equation (for problems of the type considered here), our methods, either through the use of Eq. (1.2) or Eq. (2.10) [each based on implementing the generalization of Eq. (3.6)], give us pointwise convergence and/or L^2 convergence (in the wavelet-reconstruction-based case).

ACKNOWLEDGMENTS

This work was supported, in part, by the National Science Foundation through the Center for Theoretical Studies of Physical Systems. Additional support from ARL-Fed Lab, Grant No. DAAL01-96-2-0001 is acknowledged.We would like to thank Professor Jean-Pierre Antoine, Professor Ingrid Daubechies, Professor Giorgio Mantica, Professor Alfred Msezane, Professor Xiao Qian Wang, and Professor Guido Weiss for useful discussions.

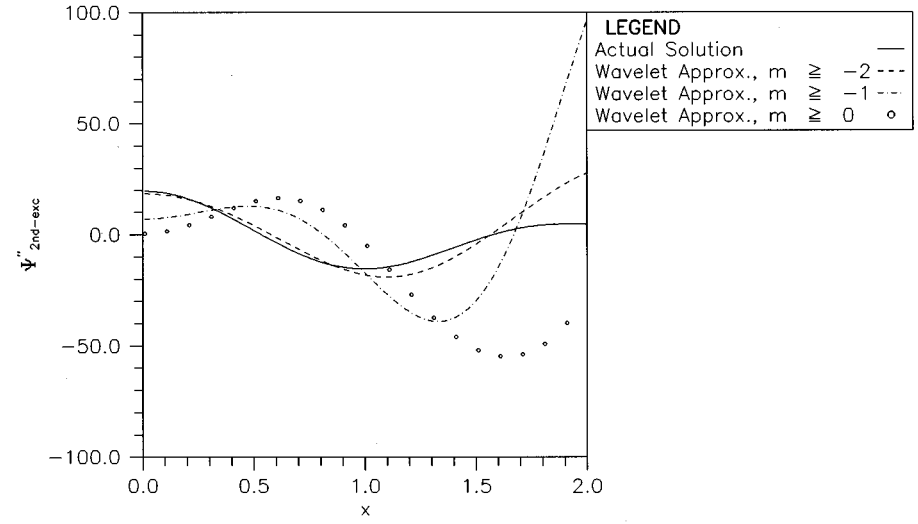

FIG. 4. $\partial_x^2\Psi_{\text{2nd-exc}}(x)$, $V(x)=x^2+x^4$.

[1] C. K. Chui, *An Introduction to Wavelets* (Academic, New York, 1992).
[2] S. Jaffard and Ph. Laurençot, *Wavelets: A Tutorial in Theory and Application*, edited by C. K. Chui (Academic, San Diego, 1992); F. Plantevin, Ph.D. thesis, Université de Provence, France, 1992 (unpublished); T. Paul, J. Math. Phys. **25**, 3252 (1984).
[3] R. Blankenbeckler, T. De Grand, and R. L. Sugar, Phys. Rev. D **21**, 1055 (1980).
[4] J. P. Killingbeck, M. N. Jones, and M. J. Thompson, J. Phys. A **18**, 793 (1985).
[5] F. M. Fernandez and J. F. Ogilvie, Phys. Lett. A **178**, 11 (1993).
[6] C. R. Handy, J. Phys. A **29**, 4093 (1996).
[7] C. R. Handy and D. Bessis, Phys. Rev. Lett. **55**, 931 (1985).
[8] C. R. Handy, D. Bessis, and T. D. Morley, Phys. Rev. A **37**, 4557 (1988).
[9] C. R. Handy, G. Sigismondi, D. Bessis, and T. D. Morley, Phys. Rev. Lett. **60**, 253 (1988).
[10] K. Chuo, T. A. Arias, J. D. Joannopoulos, and P. K. Lam, Phys. Rev. Lett. **71**, 1808 (1993).
[11] S. Wei and M. Y. Chou, Phys. Rev. Lett. **76**, 2650 (1996).
[12] C. J. Tymczak and X. Q. Wang (unpublished).
[13] A. Grossmann and J. Morlet, SIAM J. Math. Anal. **15**, 723 (1984).
[14] S. Mallat, Trans. Am. Math. Soc. **135**, 69 (1989).
[15] I. Daubechies, IEEE Trans. Theory **36**, 961 (1990).
[16] I. Daubechies, *Ten Lectures on Wavelets* (Society for Industrial and Applied Mathematics, Philadelphia, PA, 1992).
[17] M. Frazier, B. Jawerth, and G. Weiss, in *Function Spaces and Application*, edited by M. Cwikel, Lecture Notes in Mathematics Vol. 1302 (Springer-Verlag, Berlin, 1988), pp. 233–246.
[18] I. Daubechies, *Advances in Spectrum Analysis and Array Processing*, edited by S. Haykin (Prentice-Hall, Englewood Cliffs, NJ, 1991), Vol. I.
[19] I. Daubechies, in *Different Perspectives on Wavelets*, edited by I. Daubechies (American Mathematical Society, Providence, RI, 1993), Vol. 47, pp. 5 and 6.
[20] M. Reed and B. Simon, *Methods of Modern Mathematical Physics* (Academic, New York, 1978), p. 206, Theorem XIII-46.
[21] J. A. Shohat and J. D. Tamarkin, *The Problem of Moments* (American Mathematical Society, Providence, RI, 1963).
[22] N. I. Akhiezer, *The Classical Moment Problem and Some Related Questions in Analysis* (Oliver and Boyd, Edinburgh, 1965).
[23] V. Chvatal, *Linear Programming* (Freeman, New York, 1983).
[24] S. E. Koonin, *Computational Physics* (Addison-Wesley, New York, 1986).
[25] M. R. M. Witwit, J. Math. Phys. **36**, 187 (1995).
[26] C. R. Handy and P. Lee, J. Phys. A **24**, 1565 (1991).